EXAFS Study of Uranyl Nitrate Dimer at High and Low Temperature

Craig E. Barnes,*,† Yongsoon Shin,† Suree Saengkerdsub,† and Sheng Dai‡

Department of Chemistry, University of Tennessee, Knoxville, Tennessee 37996-1600, and Chemical Technology Division, Oak Ridge National Laboratory, P.O. Box 2008, Oak Ridge, Tennessee 37831-6181

Received May 7, 1999

Introduction

X-ray absorption spectroscopy (XAS) has become an increasingly important technique for the study and characterization of metal species in materials, heterogeneous catalysts, and bioinorganic substrates.[1] More recently, a number of environmental applications have also been reported in which information concerning the local coordination sphere around transuranium elements has been obtained from both near edge (XANES) and fine structure (EXAFS) studies.[2]

One of the particular strengths of EXAFS spectroscopy is the ability to provide information on the existence of other metal atoms in the vicinity of an absorber atom.[3] Distance and coordination number (CN) information for a shell of metal backscatterers may be used to propose structural models for the overall size and shape of a cluster or the extent of metal complex aggregation in amorphous matrixes and the presence and identities of ligands bridging metal ions. We have recently shown that the observation and modeling of long-range, metal backscatterers which are not directly bonded to the absorber can be made difficult by vibrational motions, which cause such components in the data to be reduced, sometimes to the point where they can no longer be detected.[4] This attenuation of a component in fine structure data due to thermal motion arises from a loss of correlated motion between the absorber and backscattering centers.[1,4]

In this paper we describe EXAFS studies on the hydroxy-bridged uranyl nitrate dimer $HIm_2[\{UO_2(\mu\text{-}OH)(NO_3)_2\}_2]$ (**1**) (HIm = imidazolium ($C_3H_5N_2$)), which we are using to model possible species found in vitreous glasses used in the safe, long-term storage of transuranic wastes.[5] We observe a pronounced temperature effect on the U···U feature in the XAS spectrum of **1**. Complete interpretation and analysis of the EXAFS observed for this complex are described.

Experimental Section

X-ray absorption data were collected for the uranium L_{III} edge (17.185 keV) on beam line 4−3 at the Stanford Synchrotron Radiation Laboratory operating at 3 GeV and 90−60 mA beam current. Monochromatic light (Si[220], detuned 50% for harmonic rejection) was collimated to 15 × 1 mm, giving rise to an estimated energy resolution of 4 eV at the edge. Transmission measurements were made at 10 K or at room temperature (294 K). Samples consisted of 20% (wt) uranyl nitrate mixed with BN powder packed in a cell between Kapton tape windows. Data were collected before and after the edge to 17*k* (total range 16.225−18.283 keV). EXAFS data were extracted from absorbance data using normal procedures, and simulation and fitting of the data to structural models were performed using the program WinXAS.[6] Final EXAFS data analysis consisted of directly fitting the raw data (k^3 weighted) to theoretical EXAFS generated from a structural model based on the reported XRD structure.[7] Theoretical phase and amplitude factors were obtained from the program FEFF-7 developed by Rehr and co-workers.[8] Fitting parameters varied in optimizing structural models were the distance *R* between the absorber and a backscatterer shell, Debye−Waller factors (σ^2), and a single adjustment to the photoelectron zero kinetic energy position, ΔE_o. Coordination numbers for each shell were fixed to the known stoichiometry of the complex in the solid state. Final simulations of the raw EXAFS data were within the maximum number of allowed modeling parameters as described by O'day et al.[9]

Results and Discussion

The structure for the uranyl nitrate μ-hydroxy-bridged dimer has been reported[7] and was used to develop theoretical scattering paths.[10] After paths which were predicted to contribute less than 20% of the maximum scattering component (U═O) are filtered out, the expected EXAFS components are (1) a shell for the two uranyl oxygen atoms, (2) a shell composed of two oxygen atoms derived from the bridging hydroxy groups, (3) a shell for the four oxygen atoms of the bidentate nitrate ligands, (4) a shell for the two nonbonded nitrogen atoms, and (5) a shell for the single nonbonded uranium atom. The distance and coordination number for each shell are summarized in Table 1.

In addition to single-scattering components, two multiple-scattering paths derived from the uranyl unit were calculated to contribute significantly to the EXAFS: a three-legged path involving backscattering off each oxygen and back to the uranium atom (U → O → O → U) and a four-legged path

† University of Tennessee.
‡ Oak Ridge National Laboratory.

(1) Bertognolli, H.; Ertel, T. S. *Angew. Chem., Int. Ed. Eng*. **1994**, *33*, 45. Gurman, S. J. Structural Information in Extended X-ray Absorption Fine Structure (EXAFS). In *Synchrotron Radiation in Biophysics*, Hassain, S. S. H., Ed.; Wiley: New York, 1990; p 8. Bart, J. C.; Valaic, G. *Adv. Catal*. **1987**, *35*, 1.
(2) Conradson, S. D. *Appl. Spectrosc*. **1998**, 252A. Clark, D. L.; Conradson, S. D.; Neu, M. P.; Palmer, P. D.; Runde W.; Drew Tait, C. *J. Am. Chem. Soc*. **1997**, *119*, 5259. Clark, D. L.; Conradson, S. D.; Ekberg, S. A.; Hess, N. J.; Neu, M. P.; Palmer, P. D.; Runde, W.; Drew Tait, C. *J. Am. Chem. Soc*. **1996**, *118*, 2089. Veirs, D. K.; Smith, C. A.; Berg, J. M.; Zwick, B. D.; Marsh, S. F.; Allen, P.; Conradson, S. D. J. *Alloys Compd*. **1994**, *213*, 328. Allen, P. G.; Bucher, J. W.; Clark, D. L.; Edelstein, N. M.; Ekberg, S. A.; Gohdes, J. W.; Hudson, E. A.; Kaltsoyannis, N.; Lukens, W. W.; New, M. P.; Palmer, P. D.; Reich, T.; Shuh, D. K.; Tait, C. D.; Zwick, B. D. *Inorg. Chem*. **1995**, *34*, 4797. Docrat, T. I.; Mosselmans, J. F. W.; Charnock, J. M.; Whiteley, M. W.; Collison, D.; Livens, F. R.; Jones, C.; Edminston, M. J. *Inorg. Chem*. **1999**, *38*, 1879.
(3) Sinfelt, J. H.; Via, G. H. l. Lytle, F. W. *Catal. Rev. Sci. Eng*. **1984**, *26*, 81. Penner-Hahn, J. E. X-ray Absorption Spectroscopy for Characterizing Metal Clusters in Proteins. Possibilities and Limitations. In Metal Clusters in Proteins; Que, L., Jr., Ed.; ACS Symposium Series 372; American Chemical Society: Washington, DC, 1988; p 28.
(4) Barnes, C. E.; Ralle, M.; Vierkötter, S. A. *J. Am. Chem. Soc*. **1995**, *117*, 5861.
(5) Cunnane, J. C.; Allison, J. M. *Sci. Basis Nucl. Waste Mgmt*. **1993**, *XVII*, 3. Schreiber, H. D.; Balazs, G. B. *Phys. Chem. Glasses* **1982**, *23*, 139. Schreiber, H. D. J. *Less-Common Met.* **1983**, *91*, 129.
(6) WinXAS (verson 1.2): Ressler, T. *J. Phys*. **1997**, *7*, 269. Ressler, T. *J. Synchrotron Rad*. **1998**, *5*, 118.
(7) Perry, D. L.; Ruben, H.; Templeton, D. H.; Zalkin, A. *Inorg. Chem*. **1980**, *19*, 1067.
(8) (a) Zabinsky, S. I.; Rehr, J. J.; Ankudinov, A.; Albers, R. C.; Elker, M. J. *Phys. Rev. B* **1995**, *53*, 2995. (b) Ankudinov, A. Ph.D. Thesis, University of Washington, 1996.
(9) O'day, P. A.; Rehr, J. J.; Zabinsky, S. I.; Brown, G. E., Jr. *J. Am. Chem. Soc.* **1994**, *116*, 2938.
(10) Perry, D. L. *Inorg. Chim. Acta* **1982**, *65*, L211.

10.1021/ic9904992 CCC: $19.00
Published on Web 02/01/2000

Table 1. Structural Data Obtained from XRD and EXAFS for $[HIm]_2[UO_2(NO_3)_2(OH)]_2$

structure element (CN)	10 K EXAFS		294 K EXAFS		XRD[a] atom separation[b] (data collected at 295 K)
	R (Å)	σ^2 (Å^2)	R (Å)	σ^2 (Å^2)	
U═O (2)	1.790	0.0014	1.797	0.0015	⟨1.77⟩ (±0.02)
U—$O_{\mu-OH}$ (2)	2.383	0.003	2.37	0.009	⟨2.36⟩ (±0.002)
U—$O_{NO_3^-}$ (4)	2.530	0.004	2.56	0.005	⟨2.55⟩ (±0.04)
U···N (2)	3.001	0.005	3.07	0.01	⟨2.98⟩ (±0.02)
U···U (1)	3.94	0.004	3.97	0.008	3.927(2)

[a] Ref 7. [b] Numbers in parentheses are esd's of the value from diffraction data or represent the spread about the mean value.

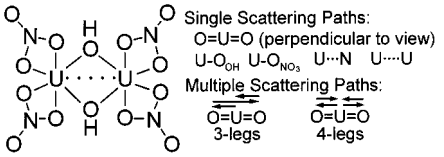

involving both oxygens and the uranium: U → O → U → O → U. These multiple-scattering paths were included in the model used to fit the data but were found to have only a small effect on the fit results. Thus, a combination of seven paths, five single-scattering and two multiple-scattering, were used from those predicted by FEFF-7.[11]

An overlay plot of the Fourier transform (FT) of the EXAFS and best fit to the data collected at 10 K are shown in Figure 1 with the actual data and fit in the inset. The dominant feature in the FT of the data arises from a shell of two uranyl oxygen atoms. The final U═O distance obtained from the data was 1.790 Å. Although significantly larger than that observed in the solid state (1.77 ± 0.02 Å), the bond distance is still within the range for these atoms obtained from XRD data at room temperature.[12] The next largest feature at low temperature was modeled as backscattering from a second uranium at a distance of 3.94 Å. As seen in the overlay of the experimental and best fit to the FT of the data, this feature corresponds very well to the second uranium atom in the dimer observed at a distance of 3.927(2) Å in the crystal. On a per atom basis, the area associated with the U···U backscattering feature in the FT of the data is almost 80% that obtained for the uranyl feature at 1.79 Å in the model. Even though there is no direct bond between the metal atoms and the U···U separation is more than 2 Å larger than the U═O distance, its contribution to the EXAFS of **1** is almost as large as that of the U═O component at low temperature.

Three other single-scattering shells of atoms were found to contribute to the observed EXAFS of **1**. In the equatorial plane of the UO_2 unit, EXAFS from the bridging hydroxy group and oxygens of the bidentate nitrate ligands interfere significantly with one another, causing shifts in the positions of their FT features. The U···N feature is observed as a small feature just beyond the second U—O shell in the FT. Because of the interference shifting, the initial identification of the oxygen shells is difficult without independent knowledge of the parameters characterizing each shell. By the same token, however, all three features are clearly present in low-temperature data and can be used as a spectral fingerprint in proposing initial models for equatorial ligation. Final parameters for these three shells agreed quite well with XRD data.

(11) Identical scattering paths distinguishing only small distance or angular variations found in the crystal structure were grouped into one average path with the appropriate degeneracy.

(12) Due to approximations in the core potential model, estimates of the Fermi level by FEFF-7 are generally a few electronvolts higher than the true position. Correcting for this discrepancy would reduce distances in the model by approximately 0.003—0.006 Å. J. J. Rehr, personal communication.

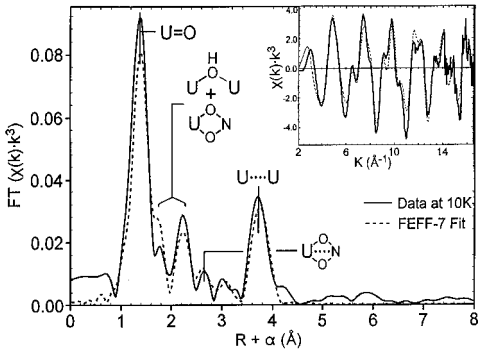

Figure 1. Overlay plots of the experimental data and theoretical fit to the Fourier transform of EXAFS for **1** at 10 K. Data are uncorrected for the EXAFS phase shift (α). Inset: Overlay plot of EXAFS and theoretical fit.

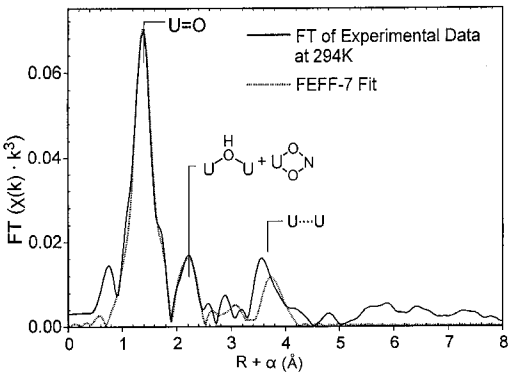

Figure 2. Overlay plots of the experimental data and theoretical fit to the Fourier transform of EXAFS for **1** at 294 K.

In the final fit to the data the sum of the areas in the FT of two multiple-scattering paths associated with the uranyl unit amounted to only 12% of the uranyl component, and these paths are barely observed in the FT of the data above the noise level. Thermal disorder in these components at 10 K should be minimized. Static disorder on the order of what is observed in the crystal structure (0.02 Å) would cause a significant broadening and larger Debye—Waller factor for these EXAFS components. However, elimination of these scattering components from the model caused a consistent and noticeable decrease in the quality of the fit to the experimental data. Therefore, they were retained in the model.

An overlay plot of the FTs of the experimental EXAFS and best fit collected at 294 K is shown in Figure 2. The results of fitting the data to the same structural model used above for the 10 K data are summarized in Table 1. The FT of the data shows that, except for the uranyl feature, all component shells in the data are significantly reduced at higher temperature. The most significant change is observed in the U···U shell, now observed at 3.97 Å. The EXAFS spectra at 294 K show a pronounced loss of fine structure in the high-k region presumably due to thermal disorder in the complex as more vibrational modes are accessed. Vibrations associated with the UO_2—$(OH)_2$—UO_2 core

are expected to have a significant effect on thermal disorder associated with the U···U component of the data, and accordingly, the Debye−Waller factor for this shell is twice as large as that observed at low temperature. Furthermore, although it appears that this feature has shifted to lower *R*, close inspection of the data reveals a pronounced asymmetry in this feature, indicating that it is now composed of two separate but overlapping components. The "new" overlapping component observed at approximately 3.5 Å arises from multiple-scattering pathways associated with the uranyl oxygens. Although these components appear to have "gained" intensity in the data at high temperature, in fact U···U scattering has actually suffered a substantial loss of intensity due to thermal disorder. The integrated area of the U···U feature in the FT is now only 15% of that arising from the uranyl oxygen shell.

The distance for the shell of uranyl oxygens increases slightly to 1.979 Å at 294 K. It has been reported that the U═O distance in uranyl complexes is affected by changes in the number and nature of the equatorial ligands.[13] Increases in the U−O bond distances involving the bridging hydroxy and bidentate nitrate ligands are expected to cause the U═O bond distance to increase. This is observed when the low- and room-temperature EXAFS data are compared. Other factors which could play a role in the analysis of the U═O shell are incomplete removal of low-*R* features due to inaccurate modeling of the background absorption (μ_o) near the edge and interference with other shells of backscatterers around the uranium.

The U−O shells for the bridging hydroxy and nitrate ligands are unresolved at room temperature, appearing as a single, asymmetric feature in the FT of the data. Nonetheless, it was possible to model this feature as two distinct shells without observing high correlations between the two sets of parameters defining each shell. No clear feature for the long-range U···N feature could be observed in room-temperature data for the complex.

In conclusion, low-temperature EXAFS of the uranyl nitrate dimer **1** may be divided into three parts: (1) the dominant U═O feature at ∼1.79 Å from the uranyl unit; (2) U−O and U··· N features between 2.3 and 3 Å arising from the belt of equatorial ligands around the uranium; (3) a long-range U···U feature at 3.94 Å. The separation of these features into distinct distance ranges lends itself both to their observation and to their detailed modeling. This generalization should apply to other uranyl and actinide complexes which possess the trans-dioxo metal unit MO_2. The data and analyses described here clearly illustrate the advantages of collecting XAS data at low temperature. Less obvious are the following observations: Long-range, nonbonded atom separations involving bridging ligands are significantly more susceptible to vibrationally derived loss of intensity in EXAFS data than shorter atom separations involving direct bonding between the absorber and backscatterer. Thus, the collection of low-temperature data is extremely important in optimizing the conditions for observing these components in EXAFS data as well as correctly modeling them. Finally, the most difficult set of components to identify in EXAFS data are derived from the equatorial ligands in uranyl complexes. At low temperature, outer sphere contributions to EXAFS from low-*Z* backscatterers are clearly observable and can be used as a spectroscopic fingerprint in identifying equatorial ligation and in subsequent modeling of these backscattering components. In data collected at room temperature, however, these components experienced a significant loss in resolution and intensity such that one critical backscattering path was no longer observed (U···N) and two others were not resolved. On the basis of these observations, the correct identification and modeling of equatorial ligation in actinyl complexes with room-temperature EXAFS data alone would in most cases be quite difficult.

Acknowledgment. This work was supported by the EMSP program of the DOE under Contract Number DE-FG07-97ER14817 between the University of Tennessee and Oak Ridge National Laboratory and by the Division of Chemical Sciences, Office of Basic Energy Sciences, U.S. Department of Energy, under Contract DE-AC05-96OR22464 with Lockheed Martin Energy Research Corp.

IC9904992

(13) (a) Denning, R. G. *Struct. Bonding* **1992**, *79*, 215. (b) Bartlett, J. R.; Cooney, R. P. *J. Mol. Struct*. **1989**, *193*, 295. (c) Metcalf, D. H.; Dai, S.; Del Cul, G. D.; Toth, L. M. *Inorg. Chem*. **1995**, *34*, 5573.